

SUPERORBITAL PERIODIC MODULATION IN WIND-ACCRETION HIGH-MASS X-RAY BINARIES FROM *Swift* BAT OBSERVATIONS

ROBIN H. D. CORBET^{1,2} AND HANS A. KRIMM^{3,4}

Draft version October 17, 2018

ABSTRACT

We report the discovery using data from the *Swift* Burst Alert Telescope (BAT) of superorbital modulation in the wind-accretion supergiant high-mass X-ray binaries 4U 1909+07 (= X 1908+075), IGR J16418-4532, and IGR J16479-4514. Together with already known superorbital periodicities in 2S 0114+650 and IGR J16493-4348, the systems exhibit a monotonic relationship between superorbital and orbital periods. These systems include both supergiant fast X-ray transients (SFXTs) and classical supergiant systems, and have a range of inclination angles. This suggests an underlying physical mechanism which is connected to the orbital period. In addition to these sources with clear detections of superorbital periods, IGR J16393-4643 (= AX J16390.4-4642) is identified as a system that may have superorbital modulation due to the coincidence of low-amplitude peaks in power spectra derived from BAT, RXTE PCA, and INTEGRAL light curves. 1E 1145.1-6141 may also be worthy of further attention due to the amount of low-frequency modulation of its light curve. However, we find that the presence of superorbital modulation is not a universal feature of wind-accretion supergiant X-ray binaries.

Subject headings: stars: individual (2S 0114+650, 1E 1145.1-6141, IGR J16393-4643, IGR J16418-4532, IGR J16479-4514, IGR J16493-4348, 4U 1909+07) — stars: neutron — X-rays: stars

1. INTRODUCTION

Superorbital modulation is seen in a variety of X-ray binaries. A review of superorbital modulation in several types of systems is presented by Kotze & Charles (2012). In some cases such as Her X-1, SMC X-1 and LMC X-4, where accretion occurs by Roche-lobe overflow via an accretion disk onto a neutron star, the mechanism driving superorbital modulation can be understood as either precession of the accretion disk (e.g. Petterson 1975) or of the neutron star (e.g. Postnov et al. 2013). Irradiation of the accretion disk by the central X-ray source provides a possible mechanism for driving disk precession (e.g. Ogilvie & Dubus 2001, and references therein). Be star systems also exhibit long timescale, possibly periodic, variability at optical wavelengths. This long timescale variability has been claimed to be correlated with orbital period (Rajoelimanana et al. 2011).

A more puzzling variety of superorbital variability was found in a supergiant high-mass X-ray binary (sgHMXB). The sgHMXBs can be broadly classified into “classical” systems, which may suffer from high levels of absorption, and supergiant fast X-ray transients (SFXTs; e.g. Blay et al. 2012; Sidoli 2013). In the sgHMXB 2S 0114+650 there are three periodicities: a \sim 9700 s neutron star rotation period, an 11.6 day orbital period, and a 30.7 day superorbital modulation (Corbet et al.

1999; Wen et al. 2006; Farrell et al. 2008). A question has been whether 2S 0114+650 is exceptional, perhaps because of its unusually long pulse period, or whether other wind-accretion HMXBs also show similar superorbital periodicities. If similar behavior is found in other systems, then this may provide a way to determine, or at least constrain, the underlying mechanism. A suggestion that the phenomenon might be more general than just the case of 2S 0114+650 came when a superorbital period was found in the sgHMXB IGR J16493-4348 (Corbet et al. 2010b).

The *Swift* BAT provides an excellent way to monitor sgHMXBs. These systems are often highly absorbed, which presents difficulties for an instrument such as the Rossi X-ray Timing Explorer (*RXTE*) All Sky Monitor (ASM) which is sensitive in the 2 - 12 keV band (Levine et al. 1996). The *Swift* BAT’s sensitivity to higher energy X-rays ($>$ 15 keV) provides a way to peer through this absorption. We present here a review of our searches of BAT light curves of sources thought to be HMXBs, in order to find additional sources that may also display superorbital modulation. In a few cases we also employ data collected from Galactic plane scans (Markwardt 2006) made with the *RXTE* Proportional Counter Array (PCA). The large effective area of the PCA enables observations to be made in the lower energy range of 2 - 10 keV. Although the PCA data cover only a limited fraction of the sky they have greater sensitivity than the *RXTE* ASM. MAXI light curves (Sugizaki et al. 2011) are not available for the majority of systems considered here.

We present here the results of a search for superorbital modulation in additional wind-accretion supergiant HMXBs. We find three new systems with clear superorbital modulation, initial reports of which were made in

¹ University of Maryland, Baltimore County, MD, USA; corbet@umbc.edu

² CRESST/Mail Code 662, X-ray Astrophysics Laboratory, NASA Goddard Space Flight Center, Greenbelt, MD 20771, USA

³ Universities Space Research Association, 10211 Wincopin Circle, Suite 500, Columbia, MD 21044, USA

⁴ CRESST/Mail Code 661, Astroparticle Physics Laboratory, NASA Goddard Space Flight Center, Greenbelt, MD 20771, USA

Corbet & Krimm (2013a,b). We also find hints of modulation in two other systems. Although the number of systems is small, three new systems plus two previously known, we note a monotonic relationship between orbital and superorbital periods. We consider possible mechanisms that might cause superorbital modulation in some, but not all, sgHMXBs.

2. DATA AND ANALYSIS

The Burst Alert Telescope (BAT) on board the *Swift* satellite (Gehrels et al. 2004) is described in detail by Barthelmy et al. (2005). It uses a 2.7 m² coded-aperture mask and a 0.52 m² CdZnTe detector array. The BAT has a wide field of view, 1.4 sr half-coded, 2.85 sr 0% coded. The pointing direction of *Swift* is driven by the narrow-field XRT and UVOT instruments on board the satellite. The BAT typically observes 50%–80% of the sky each day. We used data from the *Swift*/BAT transient monitor (Krimm et al. 2006, 2013) covering the energy range 15 - 50 keV, and selected data with time resolution of *Swift* pointing durations. The transient monitor data are available shortly after observations have been performed. The light curves considered here cover the time range of MJD 53,416 to 56,452 (2005-02-15 to 2013-06-09). The light curves of some sources, not including the ones discussed in detail here, were more recently added to the analysis and hence have shorter durations. BAT light curves are also available from the catalogs such as described by Tueller et al. (2010). However, the most recent BAT catalog is from 70 months of data (Baumgartner et al. 2012) and the transient monitor light curves are hence of longer duration. The transient monitor light curves generally cover more than 3000 days, approximately 50% longer than the 70-month catalog light curves.

We used only data for which the data quality flag (“DATA_FLAG”) was set to 0, indicating good quality. In addition, we found that even data flagged as “good” were sometimes suspect. In particular we identified a small number of data points with very low fluxes and implausibly small uncertainties. We therefore removed these points from the light curves. A total of 1244 light curves were available, this includes 106 blank fields that are used for test purposes.

To search for periodic modulation in the light curves, we calculated discrete Fourier transforms (DFTs) of all available light curves. We calculated the DFTs for a frequency range which corresponds to periods of between 0.07 days to the length of the light curves - i.e. generally ~3000 days. The contribution of each data point to the power spectrum was weighted by its uncertainty using the “semi-weighting” technique (Corbet et al. 2007a,b). This takes into account both the error bars on each data point and the excess variability of the light curve. Scargle (1989) notes that the weighting of data points in a power spectrum can be compared to combining individual data points. In this way, the use of semi-weighting is analogous to combining data points using the semi-weighted mean (Cochran 1937, 1954). We oversampled the DFTs by a factor of five compared to their nominal resolution. Calculations of the significance of peaks seen are expressed in terms of false alarm probability (FAP; Scargle 1982) which takes into account the DFT oversampling. Uncertainties in periods are generally derived using the

expression of Horne & Baliunas (1986). In the figures showing power spectra we mark in “white noise” 99.9% and 99.99% significance levels. However, many sources exhibit noise continua which are not “white”. In our calculations of FAP, we therefore determined local noise levels by fitting the continuum power levels in a narrow frequency range around each peak of interest.

3. SOURCES WITH PREVIOUSLY REPORTED PERIODIC SUPERORBITAL MODULATION

3.1. *2S 0114+650*

2S 0114+650 is an unusual HMXB system that has an exceptionally long pulse period of ~9700 s (e.g. Corbet et al. 1999). There has been controversy over the spectral classification of the mass donor, but Reig et al. (1996) derive a spectral type of B1 Ia. From optical radial velocity measurements, Grundstrom et al. (2007) determine an orbital period of 11.5983 ± 0.0006 days and a moderate eccentricity of 0.18 ± 0.05 . The orbital period is also seen in the RXTE ASM light curve (Corbet et al. 1999; Wen et al. 2006). A 30.7 ± 0.1 day superorbital period was found by Farrell et al. (2006) from *RXTE* ASM observations, and the period was later refined to 30.75 ± 0.03 days by Wen et al. (2006). Farrell et al. (2008) performed extensive *RXTE* PCA observations covering approximately 2 cycles of the superorbital period. Although Farrell et al. (2008) found variations in the X-ray absorption on the orbital period, they found no such changes over the superorbital period. However, a significant increase in the photon index of the power-law model used to fit the X-ray spectrum was reported at the minimum flux phase of the superorbital period. Farrell et al. (2008) concluded that the superorbital modulation was due to mass-accretion rate variations, although the mechanism causing this could not be determined.

The power spectrum of the BAT light curve of 2S 0114+650 is shown in Figure 1, both the orbital and superorbital periods are strongly detected, with the superorbital period being stronger than the orbital modulation. We determine orbital and superorbital periods of 11.591 ± 0.003 and 30.76 ± 0.03 days respectively. The BAT light curve of 2S 0114+650 folded on the orbital and superorbital periods is shown in Figure 2. For consistency with the work of Farrell et al. (2008) the light curve folded on the superorbital period uses a definition of phase zero as the time of minimum flux. However, for the other sources considered in this paper we use the time of maximum flux as phase zero. Both the orbital and superorbital modulations are quasi-sinusoidal and no evidence for an eclipse is seen in the light curve folded on the orbital period.

3.2. *IGR J16493-4348*

IGR J16493-4348 was discovered by Grebenev et al. (2005) and subsequent X-ray observations suggested that the source is an X-ray binary (Hill et al. 2008). Nespoli et al. (2010) classified the infrared counterpart as a B0.5 I supergiant. A 6.8 day orbital period was independently found by Corbet et al. (2010b) and Cusumano et al. (2010) using BAT 54 month survey data with the two groups finding periods of 6.7906 ± 0.0020 and 6.782 ± 0.005 days respectively. The BAT modulation was interpreted by Cusumano et al. (2010) as show-

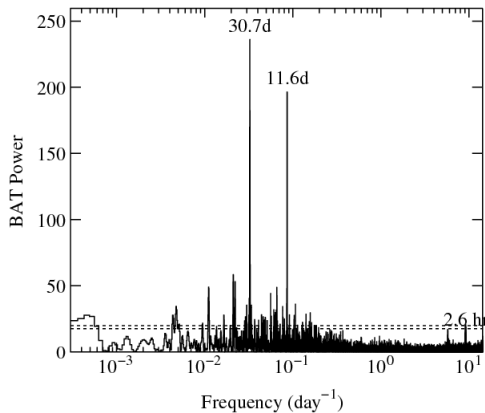


Figure 1. Power spectrum of the BAT light curve of 2S 0114+650. Note that the superorbital peak at 30.7 days is stronger than the orbital modulation at 11.6 days. The horizontal dashed lines indicate “white noise” 99.9% and 99.99% significance levels.

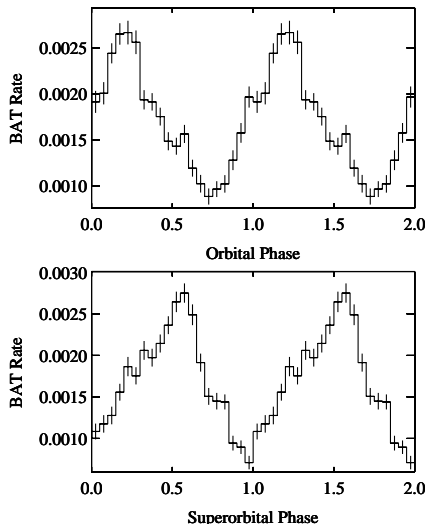


Figure 2. Swift BAT light curve of 2S 0114+650 folded on its orbital period (top) and folded on its superorbital period (bottom). The period values are given in Table 1. Phase zero for the orbital period is the time of periastron passage from Grundstrom et al. (2007) and is MJD 51,824.8. Phase zero for the superorbital period is the time of minimum flux from Farrell et al. (2008) and is MJD 53,488. We note that this definition of phase zero differs from the other sources considered in this paper where phase zero for the superorbital modulation is defined as the time of maximum flux.

ing the presence of an eclipse. Corbet et al. (2010b) confirmed the orbital period using PCA Galactic plane scan data which gave an orbital period of 6.7851 ± 0.0016 days. In addition, Corbet et al. (2010b) noted the presence of a 20.07 ± 0.02 day superorbital period in the BAT data which was confirmed by modulation at 20.09 ± 0.02 days in the PCA observations. Pointed *RXTE* PCA observations revealed a ~ 1093 s pulse period (Corbet et al. 2010c), and pulse timing with the PCA yielded a mass function of $14.0 \pm 2.3 M_{\odot}$ (Pearlman et al. 2013) which confirms the interpretation of IGR J16493-4348 as a supergiant HMXB.

The power spectrum of the BAT light curve of IGR

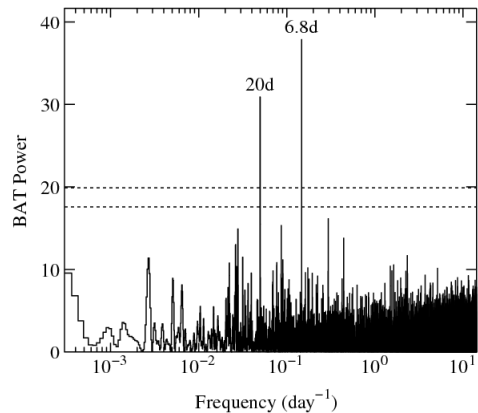


Figure 3. Power spectrum of the BAT light curve of IGR J16493-4348.

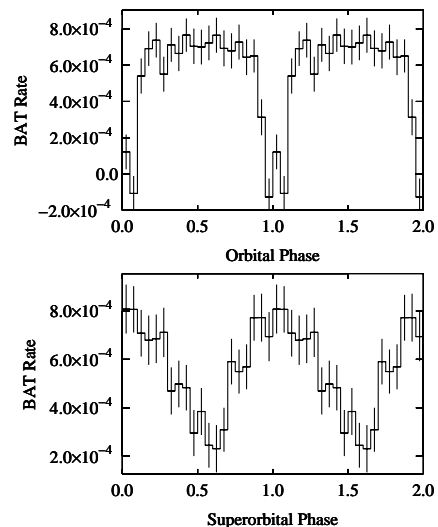


Figure 4. Swift BAT light curve of IGR J16493-4348 folded on its orbital period (top) and folded on its superorbital period (bottom). Phase zero for the orbital light curve corresponds to the center of the eclipse and is MJD 54,175.92 (Cusumano et al. 2010). Phase zero for the superorbital light curve corresponds to the time of maximum flux and is MJD 54,265.1 (Corbet et al. 2010b).

J16493-4348 is shown in Figure 3. This clearly shows the presence of the already known orbital and superorbital periods. However, the statistical significances of the periods are somewhat less than previously found from the BAT 54-month catalog data and the FAPs were $\sim 10^{-6}$ and 0.04 respectively. We refine the period measurements to be 6.782 ± 0.001 and 20.07 ± 0.01 days for the orbital and superorbital periods respectively. The BAT light curve of IGR J16493-4348 folded on the orbital and superorbital periods is shown in Figure 4. The orbital modulation shows the presence of an eclipse, while the superorbital modulation is quasi-sinusoidal.

4. SOURCES WITH NEW DETECTIONS OF PERIODIC SUPERORBITAL MODULATION

4.1. IGR J16418-4532

Chaty et al. (2008) determined that the optical coun-

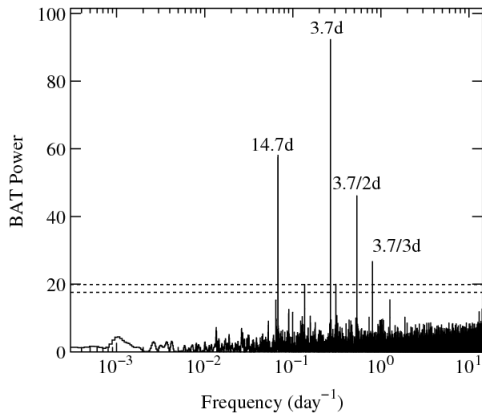


Figure 5. Power spectrum of the BAT light curve of IGR J16418-4532.

terpart of IGR J16418-4532 is probably an OB supergiant. Rahoui et al. (2008) fitted the spectral energy distribution of the likely 2MASS counterpart and found that this was consistent with an O/B massive star classification with a best fit spectral type of O8.5, although the luminosity type could not be determined. IGR J16418-4532 exhibits large flux variability, classifying it as an SFXT (Romano et al. 2011, 2012; Sidoli et al. 2012). Pulsations from the source were discovered by Walter et al. (2006) and refined to a period of 1212 ± 6 s by Sidoli et al. (2012). A 3.74 day orbital period has been found for IGR J16418-4532 from *RXTE* ASM and *Swift* BAT observations (e.g. Corbet et al. 2006; Levine et al. 2011). *INTEGRAL* and *XMM-Newton* observations of IGR J16418-4532 are discussed by Drave et al. (2013a).

The power spectrum of the BAT light curve of IGR J16418-4532 (Figure 5) shows modulation at the 3.74 day orbital period and the second and third harmonics of this. In addition the power spectrum shows a peak near 14.7 days with an FAP of $< 10^{-6}$. The light curve folded on this period (Figure 6) shows an approximately sinusoidal modulation. From a sine wave fit to the light curve we obtain:

$$T_{max} = \text{MJD } 55,994.6 \pm 0.4 + n \times 14.730 \pm 0.006$$

where T_{max} is the time of maximum flux.

The full amplitude of the modulation, defined as (maximum - minimum)/ mean flux, from the sine fit is approximately 70%. From the fundamental of the orbital peak in the power spectrum we determine an orbital period of 3.73834 ± 0.00022 days, while the second harmonic yields 3.73886 ± 0.00014 days. This is consistent with the period of $3.73886 + 0.00028, -0.00140$ days given by Levine et al. (2011). The BAT light curve of IGR J16418-4532 folded on the orbital period is also shown in Figure 6 and this shows the presence of an eclipse.

4.2. IGR J16479-4514

IGR J16479-4514 is an SFXT with a rather short orbital period of near 3.3 days with periods of 3.3194 ± 0.0010 and 3.3193 ± 0.0005 days determined by Jain et al. (2009) and Romano et al. (2009), respectively, using *Swift* BAT data in both cases. The folded light

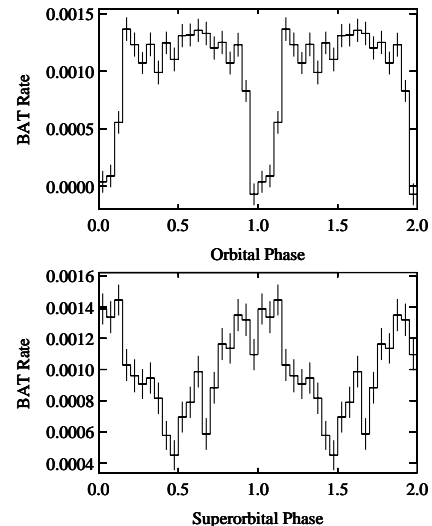


Figure 6. *Swift* BAT light curve of IGR J16418-4532 folded on its orbital period (top), and folded on its superorbital period (bottom). The period values are given in Table 1. Phase zero for the orbital period corresponds to the time of minimum flux and is MJD 52,735.84 (Levine et al. 2011). For the superorbital period phase zero corresponds to the time of maximum flux and is MJD 55,994.6 (Section 4.1).

curve shows the presence of X-ray eclipses. The mass donor has a spectral type of O8.5I (Chaty et al. 2008; Rahoui et al. 2008) or O9.5 Iab (Nespoli et al. 2008). No X-ray pulsations have yet been reported.

The power spectrum of the BAT light curve (Figure 7) shows modulation at the 3.32 day orbital period and harmonics of this. From the fundamental we determine an orbital period of 3.3199 ± 0.0005 days. In addition to this, peaks are seen near 11.9 days and its second harmonic. The FAP of the harmonic is 0.0006 while that of the fundamental is 0.05. The second harmonic is stronger than the fundamental and from this we derive a superorbital period of 11.880 ± 0.002 days. The period determined from the fundamental is consistent with this at 11.871 ± 0.005 days. The BAT light curve of IGR J16479-4514 folded on the orbital and superorbital periods is shown in Figure 8. An eclipse is clearly seen in the light curve folded on the orbital period. The light curve folded on the superorbital period shows a relatively sharp rise from minimum to maximum followed by a plateau. The time of minimum flux is approximately MJD $55,993 \pm 1.0$ with maximum flux occurring approximately 0.25 in phase after this. The full amplitude of the modulation is approximately 130%.

4.3. 4U 1909+07 (X 1908+075)

Wen et al. (2000) found a 4.400 ± 0.001 day orbital period for the X-ray binary 4U 1909+07 using *RXTE* ASM observations. X-ray pulsations with a period of 605 s were found with the *RXTE* PCA by Levine et al. (2004) and from a pulse arrival time analysis they found the orbit to be circular with an orbital period of 4.4007 ± 0.0009 days and derived a mass function of $6.1 M_{\odot}$. Although Levine et al. (2004) proposed that the primary might be a Wolf-Rayet star, Morel & Grosdidier (2005) identified a likely near-IR candidate which they proposed to be a late O-type supergiant. Levine et al. (2004)

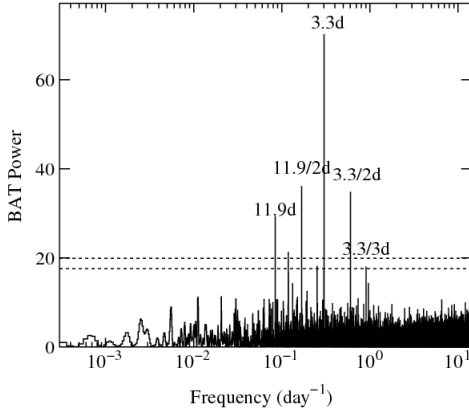


Figure 7. Power spectrum of the BAT light curve of IGR J16479-4514.

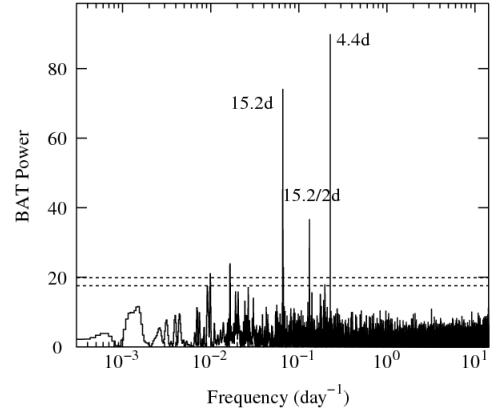


Figure 9. Power spectrum of the BAT light curve of 4U 1909+07.

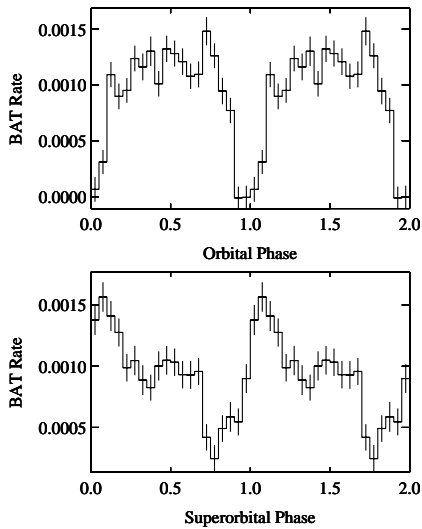


Figure 8. Swift BAT light curve of IGR J16479-4514 folded on its orbital period (top) and folded on its superorbital period (bottom). The period values are given in Table 1. Phase zero for the orbital period is the center of the eclipse and is MJD 54,547.05 (Bozzo et al. 2009). Phase zero for the superorbital period corresponds to maximum flux and is MJD 55,996 (Section 4.2).

found large orbital phase dependence of the X-ray absorption. The orbital period was further refined with additional ASM observations to 4.4005 ± 0.0004 days by Wen et al. (2006).

The power spectrum of the BAT light curve of 4U 1909+07 (Figure 9) shows strong modulation at the orbital period and we derive a period of 4.4003 ± 0.0004 days. In addition, significant modulation at a superorbital period near 15.2 days ($FAP \sim 10^{-5}$) and the second harmonic of this are seen. Combining the detections at the fundamental and second harmonic, we determine a period of 15.180 ± 0.003 days.

As expected from the presence of harmonics in the power spectrum, the light curve folded on the superorbital period (Figure 10) shows a multi-peaked profile. The minimum is somewhat more clearly defined than the maximum. From an inspection of the folded light curve,

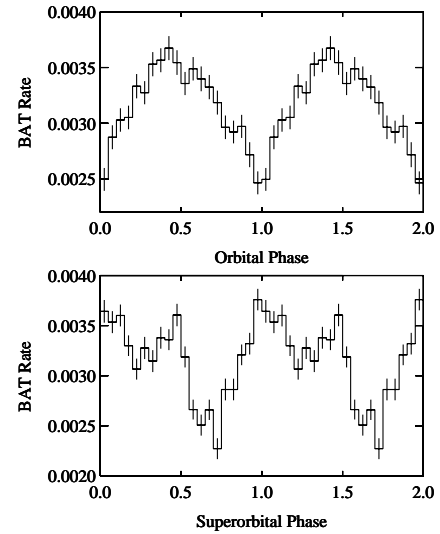


Figure 10. Swift BAT light curve of 4U 1909+07 folded on its orbital period (top) and folded on its superorbital period (bottom). The period values are given in Table 1. Phase zero for the orbital period is the time of superior conjunction from Levine et al. (2004) and is MJD 52,631.383. Phase zero for the superorbital period is the time of maximum flux and is MJD 56,004 (Section 4.3).

the minimum occurs at approximately MJD $55,999 \pm 1.5$. The time of maximum flux occurs about 0.35 in phase after the minimum. The amplitude of the modulation, defined as $(\text{maximum} - \text{minimum}) / \text{mean flux}$ is approximately 50%. The BAT light curve folded on the orbital period is shown in Figure 10. This shows a quasi-sinusoidal modulation with no evidence for the presence of an eclipse.

5. PROPERTIES OF SELECTED OTHER SGHMXBS

For comparison with the sgHMXB systems discussed above where superorbital modulation is seen, we present here examples of systems where there is no strong superorbital modulation, and two examples of systems which appear to be weak candidates for also possessing superorbital modulation.

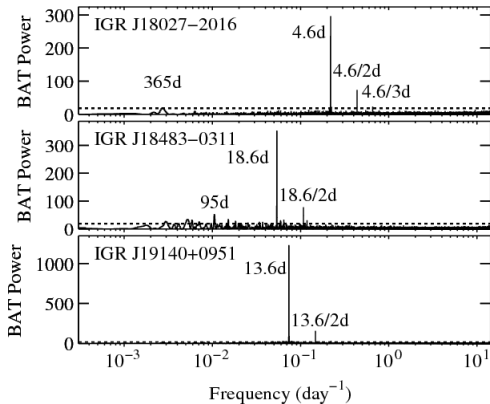


Figure 11. Power spectra of the BAT light curves of IGR J18027-2016 (top), IGR J18483-0311 (middle), and IGR J19140+0951 (bottom). The horizontal dashed lines indicate “white noise” 99.9% and 99.99% significance levels..

5.1. Examples of Systems with Strong Orbital Modulation but Lacking Superorbital Modulation

The Swift BAT set of light curves includes a number of other sgHMXBs. However, the majority of these do not show evidence for superorbital modulation. As examples we discuss here three systems. We choose “IGR” systems which are typically rather hard sources and so suitable for study with the BAT. The examples selected here all have very significant orbital modulations of their light curves which have previously been reported.

5.1.1. IGR J18027-2016 (= SAX J1802.7-2017)

IGR J18027-2016 (= SAX J1802.7-2017) has a pulse period of 139.6s (Augello et al. 2003) and pulse arrival time analysis suggested a ~ 4.6 day orbital period. From a timing analysis Hill et al. (2005) refined this to 4.5696 ± 0.0009 days. The spectral type of the mass donor has been proposed to be B1 Ib (Torrejón et al. 2010) and B0-B1 I (Mason et al. 2011), thus making it an sgHMXB. The power spectrum of the BAT light curve of IGR J18027-2016 (Figure 11, bottom panel) is very flat with the exception of the orbital period and its second and third harmonics, together with a small peak corresponding to a period of one year.

5.1.2. IGR J18483-0311

IGR J18483-0311 is an SFXT with an early B supergiant optical counterpart (Rahoui & Chaty 2008). Orbital modulation is seen at a period near 18.55 days in RXTE ASM (Levine et al. 2011), BAT (Jain et al. 2009) and INTEGRAL observations (Sguera et al. 2007). This source also has a 21 s pulse period (Sguera et al. 2007). The power spectrum of the BAT light curve of IGR J18483-0311 (Figure 11, middle panel) shows strong modulation at the orbital period and the second harmonic of this. The power spectrum exhibits somewhat larger “noise” at intermediate frequencies. A small non-statistically significant ~ 95 day bump is the third highest peak.

5.1.3. IGR J19140+0951 (= IGR J19140+098)

IGR J19140+0951 (= IGR J19140+098) was discovered with INTEGRAL (Hannikainen et al. 2004) and a 13.558 ± 0.004 day period was found from RXTE ASM and Swift BAT observations (Corbet et al. 2004). From infrared observations the optical counterpart was determined to be a B0.5 supergiant (Hannikainen et al. 2007), later refined to B0.5 Ia by Torrejón et al. (2010). No pulsations have yet been reported from this source despite INTEGRAL and RXTE PCA observations (Prat et al. 2008). The power spectrum of the BAT light curve of IGR J19140+0951 (Figure 11, top panel) shows an extremely flat power spectrum with the exception of strong peaks at the orbital period and the second harmonic of this.

5.2. Sources of Potential Superorbital Interest

Although the presence of superorbital periods in sgHMXBs does not appear to be ubiquitous, we can examine the power spectra of other wind-accretion HMXBs for the possible presence of superorbital periods under the assumption that the apparent correlation between orbital period and superorbital periods discussed in Section 6.3 is indeed correct. This then yields a restricted frequency range to be searched for superorbital modulation.

5.2.1. 1E 1145.1-6141

The spectral type of the primary of 1E 1145.1-6141 was found to be B2 Iae by Hutchings et al. (1981) and Densham & Charles (1982). The pulse period is ~ 297 s and pulse timing enabled Ray & Chakrabarty (2002) to determine a 14.365 ± 0.002 day orbital period with a modest eccentricity of 0.20 ± 0.03 . Ray & Chakrabarty (2002) report that no eclipse was seen. No detection of orbital modulation of the X-ray flux from RXTE ASM observations is reported in the papers of Wen et al. (2006) and Levine et al. (2011). However, Corbet et al. (2007b) reported detection of the orbital period of 1E 1145.1-6141 in Swift BAT data with the presence of flares at both periastron and apastron. The presence of flares at apastron is also reported from INTEGRAL observations by Ferrigno et al. (2008).

For 1E 1145.1-6141, the strongest peak in the power spectrum of the BAT light curve (Figure 12) is at the second harmonic of the 14.4 day orbital period and the second highest peak is at the orbital period itself. The blind-search FAPs of the fundamental and second harmonic peaks would be 0.1 and $\sim 10^{-5}$ respectively. The much lower significance of the fundamental is due to the increase in continuum power at lower frequencies. From the second harmonic we derive an orbital period of 14.365 ± 0.003 days, which is the same as that derived by Ray & Chakrabarty (2002) from pulse timing. The peak at the fundamental yields a period of 14.373 ± 0.007 days, which is also consistent, although with a somewhat larger uncertainty.

The BAT light curve folded on the orbital period (Figure 13) shows a double-peaked profile with maxima at periastron and apastron based on the ephemeris of Ray & Chakrabarty (2002). The third and the fourth highest peaks in the power spectrum are at periods of 67.8 ± 0.2 (equivalent to 135.6 ± 0.4 , if regarded as a second harmonic) and 131.4 ± 0.8 days. The very low FAP of 0.2 of the ~ 68 day peak means that this is not a

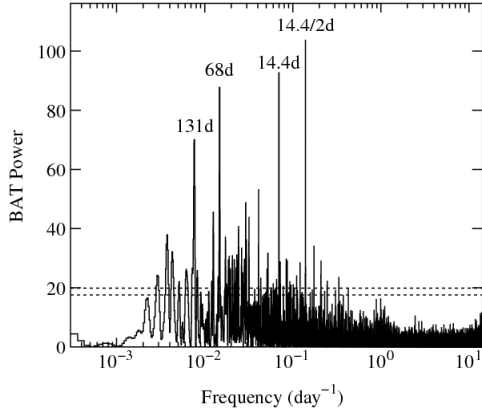


Figure 12. Power spectrum of the BAT light curve of 1E 1145.1-6141.

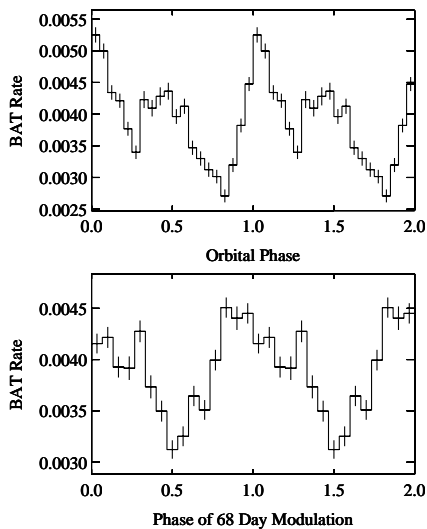


Figure 13. Swift BAT light curve of 1E 1145.1-6141 folded on its orbital period (top) and folded on a 67.8 day period (bottom). For the orbital period phase zero corresponds to the time of periastron passage (MJD 51,008.1) determined by Ray & Chakrabarty (2002). For the 68 day modulation, phase zero corresponds to the time of maximum flux from a sine wave fit to the BAT light curve and is MJD 55,142.4 (Section 5.2.1).

strong candidate for a superorbital period. However, the large amount of variability in the light curve compared to the orbital modulation makes this a potentially interesting system to continue to monitor. From a sine wave fit to the BAT light curve, we derive an epoch of maximum flux for the 68 day modulation of MJD $55,142.4 \pm 0.6$. The BAT light curve folded on the 68 day period is shown in Figure 13.

5.2.2. IGR J16393-4643 (= AX J16390.4-4642)

The 910 s X-ray pulsar IGR J16393-4643 was reported by Thompson et al. (2006) to have a 3.7 day orbital period from a pulse timing analysis, although other solutions with orbital periods of 50.2 and 8.1 days could not be excluded. Thompson et al. (2006) proposed, on the basis of their orbital parameters, that IGR J16393-

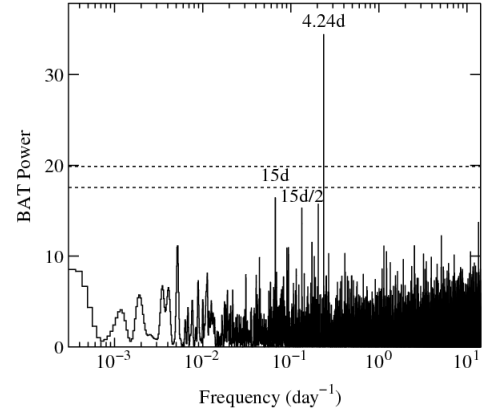


Figure 14. Power spectrum of the BAT light curve of IGR J16393-4643.

4643 is a supergiant wind-accretion powered HMXB. Nespoli et al. (2010) instead suggested that this is a symbiotic X-ray binary with a 50 day period. However, *Swift* BAT and PCA Galactic plane scan observations clearly showed the system to have a 4.2 day orbital period (Corbet et al. 2010a) which is consistent with an interpretation of the system as an sgHMXB. The periods obtained from the BAT and PCA were 4.2368 ± 0.0007 and 4.2371 ± 0.0007 days respectively.

Bodaghee et al. (2012) obtained a precise position for IGR J16393-4643 using a Chandra observation, which excluded a previously proposed counterpart that had led to the symbiotic classification by Nespoli et al. (2010), and instead suggested that the correct counterpart to IGR J16393-4643 might be a distant reddened star.

The 4.2 day orbital period of IGR J16393-4643 is similar to the 4.4 day orbital period of 4U 1909+07 which has a superorbital period of 15.2 days. If there is indeed a relationship between superorbital and orbital periods, as discussed in Section 6.3, a superorbital period of ~ 15 days would thus be predicted.

The strongest peak in the power spectrum of the updated *Swift* BAT light curve (Figure 14) is at the orbital period with a value of 4.2380 ± 0.0005 days. The second highest peak in the power spectrum (Figures 14 and 15) is at a period near 15 days at 14.99 ± 0.01 days, and there is another peak at half this period. The possible second harmonic is at a period of 7.485 ± 0.002 days, equivalent to a fundamental period of 14.971 ± 0.005 days if regarded as a harmonic. However, the “blind search” FAPs of both peaks, even restricting ourselves to a search of periods longer than the orbital period, are very high at $\sim 17\%$ and $\sim 7\%$ for the 15 and 15/2 day peaks respectively. From a sine wave fit to the BAT light curve, with the period held fixed at 14.99 days, we obtain an epoch of maximum flux of MJD $55,092.6 \pm 0.4$. The BAT light curve of IGR J16393-4643 folded on the orbital period and the possible 14.99 day period are shown in Figure 16. The folded profile on the 14.99 day period suggests any modulation may not be perfectly sinusoidal, with the maximum slightly preceding the value predicted by the sine wave fit. The light curve folded on the orbital period suggests the presence of an eclipse.

We therefore also investigated the PCA Galactic plane

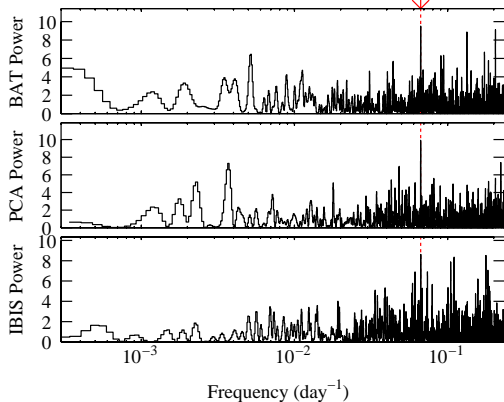


Figure 15. Power spectra of Swift BAT (top), RXTE PCA Galactic Plane scan (middle) and *INTEGRAL* (bottom) light curves of IGR J16393-4643 for periods longer than the orbital period. The vertical dashed red lines and the arrow mark the possible superorbital period.

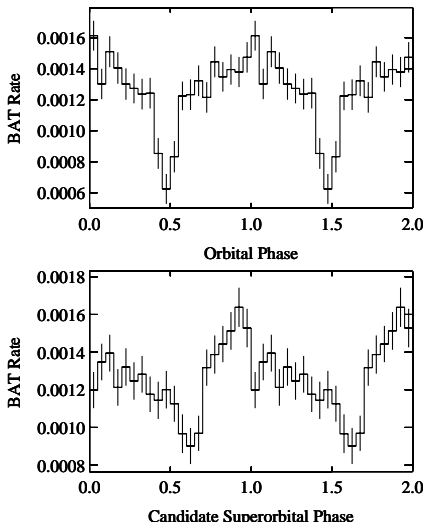


Figure 16. Swift BAT light curve of IGR J16393-4643 folded on its orbital period (top) and folded on its possible superorbital period (bottom). Period values are given in Table 1. Phase zero for the orbital period is time of maximum flux from Corbet et al. (2010a) (MJD 54,352.50) and for the possible superorbital period it is MJD 55,092.6, the epoch of maximum flux from a sine wave fit to the BAT light curve (Section 5.2.2)

scans of this source obtained between MJD 53163 and 55863 (2004-06-07 and 2011-10-29). This is 566 days longer than the light curve used in Corbet et al. (2010a). The PCA data yield an orbital period of 4.2376 ± 0.0005 days, consistent with our updated BAT result. In the power spectrum of the PCA scan observations (Figure 15), the largest peak for periods longer than the orbital period is at 14.99 ± 0.01 days, consistent with the possible BAT period.

We next examined the *INTEGRAL* light curve of IGR J16393-4643 that we obtained from the Heavens service of the ISDC. This covers a time range of MJD 52,650 to 55,856 (2003-01-11 to 2011-10-22) although with only very sparse sampling. This limited sampling yields large

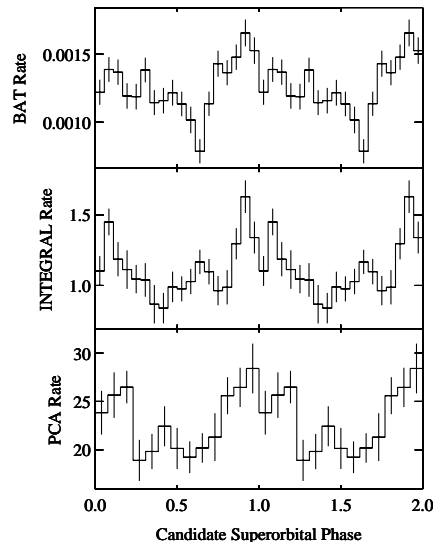


Figure 17. Swift BAT (top), *INTEGRAL* IBIS (middle) and RXTE PCA scan (bottom) light curves of IGR J16393-4643 folded on its possible superorbital period. Phase zero is MJD 55,092.6, the epoch of maximum flux from a sine wave fit to the BAT light curve (Section 5.2.2)

amounts of artifacts in the power spectrum of the light curve. For example, the 4.2 day orbital period is not the strongest peak. However, examining the peak nearest the orbital period yields a value of 4.2382 ± 0.0006 , consistent with the periods derived from the BAT and PCA observations. The *INTEGRAL* power spectrum for periods longer than the orbital period (Figure 15) also shows a small peak near 15 days. This has a value of 14.98 ± 0.01 days, which is consistent with the periods obtained from the BAT and PCA observations.

The BAT, PCA, and *INTEGRAL* data folded on the possible superorbital period derived from the BAT data are shown in Figure 17. The three light curves appear to have roughly coincident maxima. While the coincidence of the periods obtained from three separate instruments is intriguing, additional data are required to confirm whether there truly is a superorbital period in this system. Such data may come from continued monitoring with the BAT, or from future missions such as the proposed Wide Field Monitor (WFM; Bozzo & LOFT Consortium 2013) on board the Large Observatory for X-ray Timing (LOFT; Feroci et al. 2012).

6. DISCUSSION

6.1. Excluding Period Artifacts

Since the presence of superorbital periods in sgHMXBs is somewhat surprising, we consider whether they could be some type of artifact. We note that they are not present in other types of systems, and there is no obvious way to create superorbital modulation in only a subset of supergiant wind accretors. Superorbital modulation in 2S 0114+650 and IGR J16493-4348 was previously seen in other detectors (*RXTE* ASM and *RXTE* PCA Galactic plane scan data respectively). In several cases there are pulse arrival time orbits that show that the orbital period really is the orbital period. In addition, Drave et al. (2013b) report that *INTEGRAL*/IBIS data

confirm the superorbital periods found for 4U 1909+07, IGR J16418-4532, and IGR J16479-4514.

The superorbital periods are rather prominent relative to the orbital periods in the BAT energy range. This appears to differ from results of lower-energy observations such as *RXTE* ASM observations of 4U 1909+07, where the orbital period is strongly detected, but the superorbital period is not seen. Similarly, for 2S 0114+650, although the superorbital period was initially detected from *RXTE* ASM data (Farrell et al. 2006), the superorbital modulation has lower amplitude than the orbital modulation in the ASM energy band. In contrast, the superorbital modulation of 2S 0114+650 is stronger than the orbital modulation in the BAT observations. One reason for this is likely to be the lower fractional modulation of the X-ray flux on the orbital period in the BAT energy range for non-eclipsing systems. For these types of systems a large component of the orbital modulation seen with lower-energy instruments is due to the changing absorption as the neutron star orbits its companion, which the BAT is relatively insensitive to.

6.2. Coherence

Superorbital modulation from Roche-lobe overflow systems is not necessarily coherent. For example, there is considerable variation in the superorbital periods of SMC X-1 (Coe et al. 2013; Wojdowski et al. 1998) and Her X-1 (Leahy & Igna 2010), although not in LMC X-4 (Hung et al. 2010). The sampling of the BAT light curves is very variable. This potentially makes it more difficult to calculate the true resolution of the power spectra. Therefore, in order to investigate the coherency of the superorbital modulation, we compared the widths of the superorbital peaks to those of the orbital peaks. This uses the assumption that the orbital modulation should be essentially periodic. We fitted Gaussian functions to the superorbital and orbital peaks in the power spectra in the five systems for which superorbital modulation is definitely observed and determined the following ratios of superorbital to orbital peak widths: 2S 0114+650, 1.05; IGR J16493-4348, 1.16; IGR J16418-4532, 0.92; IGR J16479-4514, 0.98; 4U 1909+07, 0.92. We therefore conclude that the superorbital modulations have very high coherence. For the two low-significance candidates we obtain ratios of superorbital to orbital peak widths of: IGR J16393-4643, 0.66; 1E 1145.1-6141, 0.89.

6.3. Relationship Between Superorbital and Orbital Periods

System parameters are summarized in Table 1, and in Figure 18 we plot superorbital period against orbital period. For the five systems with definite superorbital modulation, the linear correlation coefficient between P_{super} and P_{orb} is 0.996 and the associated probability of obtaining this level of correlation from a random data set is 0.03%. Because this possible correlation comes from such a small number of systems, a determination whether this possible dependence of superorbital period on orbital period is correct requires the candidate superorbital period in IGR J16393-4643 to be investigated with additional data, and further superorbital periods must be found in other systems. For the five systems the best linear fit for superorbital periods vs. orbital period has parameters

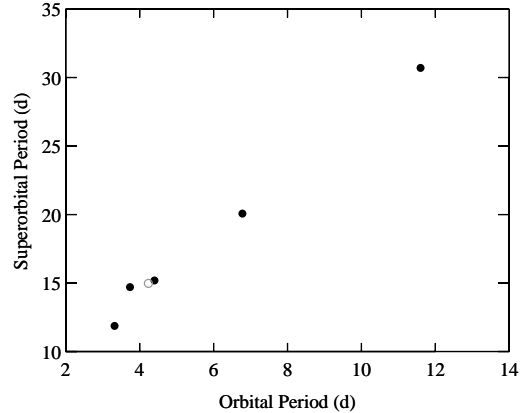


Figure 18. Superorbital period plotted against orbital period for the wind-accretion HMXBs discussed in the text. Statistical uncertainties on period measurements are smaller than symbol sizes. The filled symbols show definite superorbital period detections. The gray open symbol marks the modulation seen in IGR J16393-4643 which is not yet considered to be a definite detection of a superorbital period.

of:

$$P_{super} = 2.2 \pm 0.1 \times P_{orb} + 5.6 \pm 0.8 \text{ days}$$

For comparison, in Figure 19 we plot superorbital period against orbital period for a wide variety of systems. These include these Roche-lobe overflow powered systems: LMC X-4 (neutron star HMXB, $P_{orb} = 1.4$ days, $P_{super} = 30.3$ days), Her X-1 (neutron star intermediate-mass system, $P_{orb} = 1.7$ days, $P_{super} = 35$ days), SMC X-1 (neutron star HMXB, $P_{orb} = 3.89$ days, $P_{super} = 56$ days), and SS 433 (black hole candidate microquasar, $P_{orb} = 13.1$ days, $P_{super} = 162.5$ days). These parameters are taken from Kotze & Charles (2012). Be star systems are also shown with their parameters taken from Rajoelimanana et al. (2011). For the Be star systems the superorbital modulation periods may be quasi-periodic rather than strictly periodic. If the mechanisms driving superorbital modulation differ between different types of object, then the different types of system could be located in different regions of this diagram. We note that the sgHMXB superorbital periods are rather short relative to their orbital periods, compared to other types of systems. This is suggestive that, as expected, a different driving mechanism may be at work in the sgHMXBs superorbital modulation compared to the other types of system.

6.4. Possible Mechanisms Driving Superorbital Modulation

We note that Farrell et al. (2008)'s extensive *RXTE* PCA observations of 2S 0114+650 showed that there were changes in absorption over the orbital period of this system, but not on the superorbital period. Farrell et al. (2008) therefore concluded that the superorbital modulation was related to variability in the mass accretion rate caused by an unknown mechanism. This is consistent with the stronger detection of superorbital periods with the BAT compared to orbital periods for non-eclipsing systems than is the case with the *RXTE* ASM (Section 6.1). The ASM is more sensitive to changes in

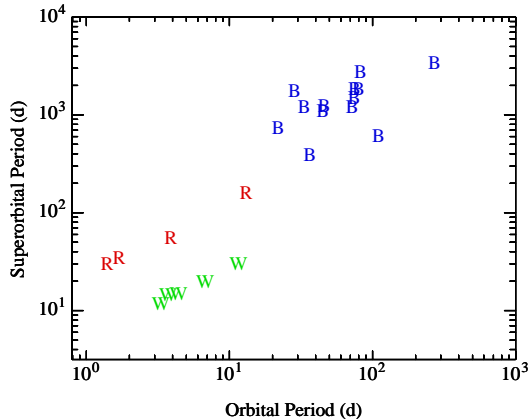


Figure 19. Superorbital period plotted against orbital period for a variety of HMXBs including both neutron star and black hole systems. “R” indicates Roche-overflow systems, “W” are the five wind-accretion systems discussed in this paper, and “B” shows Be star system parameters taken from Rajoelimanana et al. (2011). The sources included as Roche-lobe overflow systems are the high-mass neutron star systems LMC X-4 and SMC X-1, the intermediate-mass neutron star system Her X-1, and the black hole candidate SS 433.

absorption over the orbital period. However, the BAT has overall better sensitivity for changes in the flux of highly-absorbed systems.

If mass-transfer rate variations are the cause of periodic superorbital modulation, then this suggests that the wind from the primary star could itself be modulated in some way by a mechanism related to the length of the orbital period. However, any satisfactory model must be able to account for the lack of superorbital variability in many systems. Thus, the modulation must be related to some parameter independent of inclination angle and whether the system is an SFXT or classical supergiant system. For example, an offset between the orbital plane and the rotation axis of the primary star, or a small orbital eccentricity, might satisfy such a requirement. The light curves folded on the superorbital periods exhibit a variety of morphologies, and so any model for the modulation must be able to account for this. We note the work of Koenigsberger et al. (2003) and Moreno et al. (2005) indicates that oscillations can be induced in non-synchronously rotating stars in binary systems on periods longer than the orbital period. As discussed by Koenigsberger et al. (2006), such oscillations result in changes in the mass-loss rate of the primary star which would cause correlated changes in the X-ray luminosity. This model may also be consistent with the lack of superorbital modulation in all systems if only a fraction of primary stars are rotating non-synchronously. However, as noted by Farrell et al. (2008), the Koenigsberger et al. (2006) model applies to circular orbits and 2S 0114+650 has a modest eccentricity of 0.2. In addition, the high coherency of the superorbital modulations seems difficult to account for with oscillations of the primary star unless there is some way to keep strict phase stability.

In principle, the presence of a third object in the systems might drive superorbital modulation. The modulation from a third body would also naturally account for the coherency of the superorbital modulation. How-

ever, the apparent correlation between superorbital and orbital periods would, if confirmed, place stringent constraints on how such multi-star systems might be formed. In addition, typically such triple body models for X-ray sources involve hierarchical systems with a distant third object (e.g. Mazeh & Shaham 1979).

7. CONCLUSION

Observations with the *Swift* BAT have shown the presence of superorbital periods in three additional sgHMXBs for a total of five definite such systems. The superorbital modulations have a variety of morphologies, ranging from approximately sinusoidal to multi-peaked profiles. However, superorbital modulation is not a ubiquitous property of sgHMXBs. With this limited set of data, a possible dependence of superorbital period on orbital period is suggested. The mechanism(s) driving such superorbital modulation remain unclear. However, possible models based on oscillations in the primary star driven by non-synchronous rotation, and three-body systems deserve further investigation. Continued monitoring of sgHMXBs in hard X-rays both with additional *Swift* BAT data and also potential new missions with high-energy X-ray sensitivity such as the LOFT WFM may reveal additional sources with superorbital periodicities.

We thank an anonymous referee for useful comments. This paper used *Swift*/BAT transient monitor results provided by the *Swift*/BAT team. The *Swift*/BAT transient monitor and H. A. K. are supported by NASA under *Swift* Guest Observer grants NNX09AU85G, NNX12AD32G, NNX12AE57G and NNX13AC75G.

REFERENCES

- Augello, G., Iaria, R., Robba, N. R., et al. 2003, *ApJ*, 596, L63
- Barthelmy, S. D., Barbier, L. M., Cummings, J. R., et al. 2005, *Space Sci. Rev.*, 120, 143
- Baumgartner, W. H., Tueller, J., Markwardt, C. B., et al. 2013, *ApJS*, 207, 19
- Blay, P., Negueruela, I., & Reglero, V. 2012, *Mem. Soc. Astron. Italiana*, 83, 251
- Bodaghee, A., Rahoui, F., Tomsick, J. A., & Rodriguez, J. 2012, *ApJ*, 751, 113
- Bozzo, E., Giunta, A., Stella, L., et al. 2009, *A&A*, 502, 21
- Bozzo, E., & LOFT Consortium 2013, arXiv:1305.4198
- Chaty, S., Rahoui, F., Foellmi, C., et al. 2008, *A&A*, 484, 783
- Cochran, W. G. 1937, *Supplement to the Journal of the Royal Statistical Society*, 4, 102
- Cochran, W. G. 1954, *Biometrics*, 10, 101
- Coe, M. J., Angus, R., Orosz, J. A., & Udalski, A. 2013, *MNRAS*, 430, 1454
- Corbet, R. H. D., Finley, J. P., & Peele, A. G. 1999, *ApJ*, 511, 876
- Corbet, R. H. D., Hannikainen, D. C., & Remillard, R. 2004, *The Astronomer's Telegram*, 269, 1
- Corbet, R., Barbier, L., Barthelmy, S., et al. 2006, *The Astronomer's Telegram*, 779, 1
- Corbet, R. H. D., Markwardt, C. B., & Tueller, J. 2007, *ApJ*, 655, 458
- Corbet, R., Markwardt, C., Barbier, L., et al. 2007, *Progress of Theoretical Physics Supplement*, 169, 200
- Corbet, R. H. D., Krimm, H. A., Barthelmy, S. D., et al. 2010a, *The Astronomer's Telegram*, 2570, 1
- Corbet, R. H. D., Barthelmy, S. D., Baumgartner, W. H., Krimm, H. A., Markwardt, C. B., Skinner, G. K., & Tueller, J. 2010b, *The Astronomer's Telegram*, 2599, 1
- Corbet, R. H. D., Pearlman, A. B., & Pottschmidt, K. 2010c, *The Astronomer's Telegram*, 2766, 1
- Corbet, R. H. D., & Krimm, H. A. 2013a, *The Astronomer's Telegram*, 5119, 1
- Corbet, R. H. D., & Krimm, H. A. 2013b, *The Astronomer's Telegram*, 5126, 1
- Cusumano, G., La Parola, V., Romano, P., et al. 2010, *MNRAS*, 406, L16
- Densham, R. H., & Charles, P. A. 1982, *MNRAS*, 201, 171
- Drave, S. P., Bird, A. J., Sidoli, L., et al. 2013a, *MNRAS*, 430, 1439
- Drave, S. P., Bird, A. J., Goossens, M. E., Sidoli, L., Sguera, V., Fionchi, M., & Bazzano, A. 2013b, *The Astronomer's Telegram*, 5131, 1
- Farrell, S. A., Sood, R. K., & O'Neill, P. M. 2006, *MNRAS*, 367, 1457
- Farrell, S. A., Sood, R. K., O'Neill, P. M., & Dieters, S. 2008, *MNRAS*, 389, 608
- Feroci, M., Stella, L., van der Klis, M., et al. 2012, *Experimental Astronomy*, 34, 415
- Ferrigno, C., Segreto, A., Mineo, T., Santangelo, A., & Staubert, R. 2008, *A&A*, 479, 533
- Gehrels, N., Chincarini, G., Giommi, P., et al. 2004, *ApJ*, 611, 1005
- Grebenev, S. A., Bird, A. J., Molkov, S. V., et al. 2005, *The Astronomer's Telegram*, 457, 1
- Grundstrom, E. D., Blair, J. L., Gies, D. R., et al. 2007, *ApJ*, 656, 431
- Hannikainen, D. C., Rodriguez, J., Cabanac, C., et al. 2004, *A&A*, 423, L17
- Hannikainen, D. C., Rawlings, M. G., Muhli, P., et al. 2007, *MNRAS*, 380, 665
- Hill, A. B., Walter, R., Knigge, C., et al. 2005, *A&A*, 439, 255
- Hill, A. B., Dean, A. J., Landi, R., et al. 2008, *MNRAS*, 385, 423
- Horne, J. H., & Baliunas, S. L. 1986, *ApJ*, 302, 757
- Hung, L.-W., Hickox, R. C., Boroson, B. S., & Vrtillek, S. D. 2010, *ApJ*, 720, 1202
- Hutchings, J. B., Crampton, D., & Cowley, A. P. 1981, *AJ*, 86, 871
- Jain, C., Paul, B., & Dutta, A. 2009, *MNRAS*, 397, L11
- Koenigsberger, G., Moreno, E., & Cervantes, F. 2003, *A Massive Star Odyssey: From Main Sequence to Supernova*, 212, 101
- Koenigsberger, G., Georgiev, L., Moreno, E., et al. 2006, *A&A*, 458, 513
- Kotze, M. M., & Charles, P. A. 2012, *MNRAS*, 420, 1575
- Krimm, H., Barbier, L., Barthelmy, S. D., et al. 2006, *The Astronomer's Telegram*, 904, 1
- Krimm, H. A., Holland, S. T., Corbet, R. H. D., Pearlman, A. B., Romano, P., Kennea, J. A., Bloom, J. S., Barthelmy, S. D., Baumgartner, W. H., Cummings, J. R., Gehrels, N., Lien, A. Y., Markwardt, C. B., Palmer, D. M., Sakamoto, T., Stamatikos, M., Ukwatta, T. N. 2013, *ApJS*, in press. arXiv:1309.0755
- Leahy, D. A., & Igna, C. D. 2010, *ApJ*, 713, 318
- Levine, A. M., Bradt, H., Cui, W., et al. 1996, *ApJ*, 469, L33
- Levine, A. M., Rappaport, S., Remillard, R., & Savcheva, A. 2004, *ApJ*, 617, 1284
- Levine, A. M., Bradt, H. V., Chakrabarty, D., Corbet, R. H. D., & Harris, R. J. 2011, *ApJS*, 196, 6
- Markwardt, C. B. 2006, *The Transient Milky Way: A Perspective for MIRAX*, 840, 45
- Mason, A. B., Norton, A. J., Clark, J. S., Negueruela, I., & Roche, P. 2011, *A&A*, 532, A124
- Mazeh, T., & Shaham, J. 1979, *A&A*, 77, 145
- Morel, T., & Grosdidier, Y. 2005, *MNRAS*, 356, 665
- Moreno, E., Koenigsberger, G., & Toledano, O. 2005, *A&A*, 437, 641
- Nespoli, E., Fabregat, J., & Mennickent, R. E. 2008, *A&A*, 486, 911
- Nespoli, E., Fabregat, J., & Mennickent, R. E. 2010, *A&A*, 516, A106
- Ogilvie, G. I., & Dubus, G. 2001, *MNRAS*, 320, 485
- Petterson, J. A. 1975, *ApJ*, 201, L61
- Pearlman, A. B., Corbet, R., & Pottschmidt, K. 2013, *American Astronomical Society Meeting Abstracts*, 221, #142.38
- Postnov, K., Shakura, N., Staubert, R., Kochetkova, A., Klochkov, D., & Wilms, J. 2013, arXiv:1307.6026
- Prat, L., Rodriguez, J., Hannikainen, D. C., & Shaw, S. E. 2008, *MNRAS*, 389, 301
- Rahoui, F., Chaty, S., Lagage, P.-O., & Pantin, E. 2008, *A&A*, 484, 801
- Rahoui, F., & Chaty, S. 2008, *A&A*, 492, 163
- Rajoleimanana, A. F., Charles, P. A., & Udalski, A. 2011, *MNRAS*, 413, 1600
- Ray, P. S., & Chakrabarty, D. 2002, *ApJ*, 581, 1293
- Reig, P., Chakrabarty, D., Coe, M. J., et al. 1996, *A&A*, 311, 879
- Romano, P., Sidoli, L., Cusumano, G., et al. 2009, *MNRAS*, 399, 2021
- Romano, P., Mangano, V., Esposito, P., et al. 2011, *The Astronomer's Telegram*, 3174, 1
- Romano, P., Mangano, V., Ducci, L., et al. 2012, *MNRAS*, 419, 2695
- Scargle, J. D. 1982, *ApJ*, 263, 835
- Scargle, J. D. 1989, *ApJ*, 343, 874
- Sguera, V., Hill, A. B., Bird, A. J., et al. 2007, *A&A*, 467, 249
- Sidoli, L., Mereghetti, S., Sguera, V., & Pizzolato, F. 2012, *MNRAS*, 420, 554
- Sidoli, L. 2013, arXiv:1301.7574
- Sugizaki, M., Mihara, T., Serino, M., et al. 2011, *PASJ*, 63, 635
- Thompson, T. W. J., Tomsick, J. A., Rothschild, R. E., in't Zand, J. J. M., & Walter, R. 2006, *ApJ*, 649, 373
- Torrejón, J. M., Negueruela, I., Smith, D. M., & Harrison, T. E. 2010, *A&A*, 510, A61
- Tueller, J., Baumgartner, W. H., Markwardt, C. B., et al. 2010, *ApJS*, 186, 378
- Walter, R., Zurita Heras, J., Bassani, L., et al. 2006, *A&A*, 453, 133
- Wen, L., Remillard, R. A., & Bradt, H. V. 2000, *ApJ*, 532, 1119
- Wen, L., Levine, A. M., Corbet, R. H. D., & Bradt, H. V. 2006, *ApJS*, 163, 372
- Wojdowski, P., Clark, G. W., Levine, A. M., Woo, J. W., & Zhang, S. N. 1998, *ApJ*, 502, 253

Table 1
Wind-Accretion sgHMXBs with Periodic Superorbital Modulation

Name	P_{orb} (days)	P_{super} (days)	P_{super}/P_{orb}	P_{spin} (s)	Spectral Type	Eccentricity	SFXT?
IGR J16479-4514	3.3199 ± 0.0005	11.880 ± 0.002 days	3.58	?	O8.5I/O9.5 Iab	?	Y
IGR J16418-4532	3.7389 ± 0.0001	14.730 ± 0.006	3.94	1212	O8.5	?	Y
4U 1909+07	4.4003 ± 0.0004	15.180 ± 0.003	3.45	605	late O	0.02 ± 0.04	N
IGR J16493-4348	6.782 ± 0.001	20.07 ± 0.01	2.96	1093	B0.5I Ia-Ib	?	N
2S 0114+650	11.591 ± 0.003	30.76 ± 0.03	2.65	~ 9700	B1 Ia	0.18 ± 0.05	N
IGR J16393-4643	4.2380 ± 0.0005	(14.99 ± 0.01)	(3.54)	910	?	?	N

Note. — The superorbital period for the system below the line is a candidate and not a definite detection. The references for system parameters are given in the individual sections on each source. The orbital and superorbital periods and their errors are derived from the BAT light curves. For some systems additional determinations of periods may be available from other work, as given in the individual source sections.